Genetic algorithm and first-principles DFT study of the high-pressure molecular ζ phase of nitrogen

James Hooper,[1] Anguang Hu,[1] Fan Zhang,[2] and Tom K. Woo[1,*]
[1]*Department of Chemistry, University of Ottawa, 10 Marie Curie, Ottawa, Canada K1N 6N5*
[2]*Defence R&D Canada-Suffield, PO Box 4000, Medicine Hat, Alberta, Canada T1A 8K6*
(Received 27 June 2009; revised manuscript received 27 August 2009; published 25 September 2009)

The phase diagram for the precursors to polymeric nitrogen, species of molecular nitrogen, is well known up to ~30 GPa. The ζ molecular phase, the supposed precursor to the highly sought polymeric nitrogen phase, has been confirmed experimentally at higher pressures but the limits of x-ray and Raman characterization techniques have made it difficult to assign its structure. We present an exhaustive computational study of the high-pressure molecular nitrogen potential-energy surface using *ab initio* density-functional theory calculations, wherein we have identified possible structures which relate to the experimental findings published thus far.

DOI: 10.1103/PhysRevB.80.104117 PACS number(s): 61.50.Ah

I. INTRODUCTION

The characterization of such unostentatious systems as homonuclear diatomic molecular solids remains a fundamental problem in the field of ultrahigh pressure materials synthesis since one often has limited x-ray diffraction data available due to the harsh experimental conditions and/or weak scattering properties of the atoms under study. High-pressure phases of molecular oxygen and nitrogen, in particular, have been actively studied. This is highlighted by the recent identification or confirmation of the structures of the elusive ε and ζ molecular oxygen phases using single-crystal x-ray diffraction data[1–4] and an ongoing debate over the nature of high-pressure phases of molecular nitrogen.[5–13] These solid molecular structures are sought because they are typically intermediates to even more interesting high-pressure phases, such as the superconducting high-pressure ζ phase of oxygen[14] or the high-energy-density polymeric form of nitrogen.[15]

The phase diagram of high-pressure molecular nitrogen has been studied extensively but attempts to elucidate the correct molecular crystal structures have proven difficult. Advances in x-ray diffraction techniques have allowed the scientific community to fully characterize the phase diagram up to pressures of ~30 GPa, but beyond this threshold the limits inherent to x-ray diffraction measurements of low-Z materials make data analysis difficult. It is well known that the ε-phase of molecular nitrogen, the highest pressure phase with a solved molecular crystal structure, undergoes a structural transformation beyond 60 GPa to the so-called ζ phase. The ζ phase is proposed to be a precursor to the cubic gauche phase, cg-N, of solid polymeric nitrogen,[16] a highly sought-after nitrogen allotrope for its potential use as a high-energy-density material. The precise molecular structure of the ζ phase is, to date, unconfirmed but could prove invaluable in understanding the limitations and feasibilities of the molecular to polymeric transition that are currently being intensely studied.

There have been a couple of different, and conflicting, analyses of the ε-ζ phase transition reported in the recent literature.[10,12] In both studies the cells were indexed as primitive orthorhombic but they have markedly different lattice parameters. To simplify further discussion, we will herein refer to the cell reported by Eremets *et al.*[12] as cell A and to the cell reported by Hemley *et al.*[10] as cell B. The a/c and a/b lattice vector ratios for the two cells are 0.83 and 1.50 versus 0.95 and 2.53 for cells A and B, respectively, suggesting that two distinct phases with different crystal structures may be involved. Furthermore, the reported space groups consistent with the observed systematic extinctions in the diffraction patterns do not agree. Specifically, the reported space groups for cell A are consistent with $P222_1$, $P2_12_12$, and $P2_12_12_1$ symmetries, while for cell B the space group has been assigned as *Pmma*. Regarding cell A, since the screw axes of the $P222_1$ space group are in the same crystallographic direction as those in the $I2_13$ space group of cg-N, $P222_1$ was selected to be the lead candidate for cell A. However, questions were raised if this space group could be one of candidates for the ζ-phase structure based on the number of measured Raman active vibronic and lattice modes.[9]

It is the goal of this study to computationally investigate the discrepancy in the reported experimental cells and explore the structure of the ζ phase by performing an exhaustive *ab initio* search of the molecular nitrogen potential-energy surface within both cells using search algorithms inspired by the genetic algorithm.[17,18] We identify structures compatible with each of the experimental cells and report possible ζ phase structures, including stability analyses.

II. PROCEDURE

A number of methodologies have been recently developed to search out the most stable crystal structures of a system at given P-T conditions, notably those based on the genetic algorithm.[17–19] These methodologies recursively generate lower-energy structures through a number of predefined operations intended to pass on favorable structural traits from generation to generation until the overall health of the population converges. These methods have recently been successfully applied to study clusters, surfaces, and high-pressure solids.[18,20–23] Among them, applications of the genetic algorithm to high-pressure polymeric nitrogen have re-

cently been reported, demonstrating its applicability to nitrogen systems.[20,24,25] We have implemented an algorithm similar to that described in Ref. 20 and in this study we apply this genetic algorithm to study the ζ molecular phase of nitrogen.

Previous genetic algorithm studies traditionally represent a crystal by a list of N atomic Cartesian coordinates,[17] requiring no prior information about the system aside from the composition and volume of the unit cell. Given that polymeric phases of nitrogen are the lowest enthalpy nitrogen allotropes by ~0.25 eV/atom in the pressure range of interest (80 and 90 GPa),[26] we adapted the procedure to allow for an efficient mapping of the potential-energy surface pertaining to molecular nitrogen. The crystal structures were represented by the Cartesian coordinates of each N_2 molecule's center of mass, along with a corresponding set of spherical coordinates to define the remaining angular degrees of freedom. For structure evolution, the number of atoms was kept constant for the duration of the procedure wherein, at each step, randomly chosen mating operations were used to combine structural motifs of two randomly chosen "parent" genes. The mating operations used in this study were the following: (i) randomly choosing a subset of molecules from each parent to make the whole offspring, (ii) taking the arithmetic averages of the molecular coordinates, (iii) taking the geometric averages of the molecular coordinates, (iv) swapping individual Cartesian coordinates (x, y, or z) among a randomly chosen subset of molecules, and (v) cutting out a cubic subsection of one parent structure and replacing that substructure with that of the other parent structure. Only one randomly chosen mating operation was chosen to generate a single offspring. If the mating procedure changes the number of molecules in the system, then N_2 molecules are randomly added or removed to obtain the correct number. Offspring structures were only added to the next generation if the atoms between any two N_2 molecules were at least 1.3 Å apart, otherwise the same mating operation was repeated. The resulting offspring structures are given a 25% chance to mutate. The mutation used in this study involved randomly selecting between one and three N_2 molecules and randomly translating, rotating, or stretching/compressing these selected molecules.

The method of evaluating the "fitness" of a candidate structure, a metric that determines how well the structure fits the desired profile, is intrinsic to the success of the genetic algorithm. We chose to determine the fitness of a given crystal structure from its derived enthalpy from first-principles density-functional theory (DFT) calculations. For all enthalpy calculations we used the Vienna *Ab-Initio* Simulation Package (VASP).[27] The projector augmented wave (PAW) method of Blöchl[28] was used to treat the core states and the nitrogen $2s$ and $2p$ electrons were treated as valence electrons with a plane-wave cutoff of 500 eV for geometry optimizations and 800 eV for energy evaluations. The gradient-corrected exchange and correlation functionals of Perdew-Burke-Ernzerhof (PBE) (Ref. 29) were used in all calculations. For energy evaluations within the genetic algorithm, the Brillouin-zone integrations were performed using $3\times3\times3$ Monkhorst-Pack grids, whereas $10\times10\times10$ meshes were used in more refined calculations for the phases selected for further study. Although costly, the density-functional level of theory is necessary to adequately describe the solid molecular nitrogen electronic structure; our calculations show that cheaper alternatives, such as force fields, are generally not transferable enough to be of value for the broad scope of the problem presented here.

We found that the search algorithm was more efficient if the fitness function was modified to penalize structures that were nonmolecular by adding a correction term for every intermolecular bond distance that was less than 1.65 Å. The correction term was taken from a harmonic potential fit to give no correction for intermolecular distances of 1.65 Å and add a 1.25 eV/atom penalty for 1.41 Å distances, this being the N-N bond distance within the polymeric cubic gauche structure.

In this study a population size of 100 individuals was utilized for each generation. The initial population was randomly generated such that all configurations possessed intermolecular atomic distances greater than 1.6 Å. New generations were created in the following manner. First, the ten lowest enthalpy structures were promoted, unperturbed, to the next generation. To generate the rest of the population, low enthalpy structures were preferentially chosen as parent structures by selecting the parent structures from a Boltzmann weighted probability distribution.[17] The exponential term stems from the calculated enthalpies scaled by an appropriate temperature to allow at least a 25% chance to select half of the promoted structures. Unphysical structures are screened out during the mating process and the remaining generated structures are loosely optimized before evaluating their fitness. The algorithm was halted when the energy of the four lowest-energy structures remained unchanged for five generations, typically running for, on average 20 generations. At least five distinct production runs were employed resulting in at least 10 000 structures being evaluated and partially optimized at the DFT level for each cell.

Phonon calculations, used to evaluate the mechanical stability of the generated phases, were done with the finite difference method with the aid of VASP and the external package FROPHO.[30] They were subsequently confirmed using forces calculated from SIESTA.[31] SIESTA calculations used a Troullier-Martins norm-conserving pseudopotential, referencing a $[He]2s^22p^3$ configuration with a 1.24 Å cutoff. Custom numerical doubled s, p_x, p_y, and p_z orbitals and d polarization orbitals were used with a real-space mesh cutoff of 200.0 Ry. A 20 Å cutoff for k-point sampling was used to construct Monkhorst-Pack grids for Brillouin-zone integration. Simulated x-ray patterns were calculated using the reflex module from the MATERIALS STUDIO® simulation package version 3.2 from Accelrys, San Diego, California.[32]

III. RESULTS AND DISCUSSION

Given the discrepancy between the reported experimental unit cells of the ζ phase, we investigated both cell A and cell B by running two distinct sets of evolutionary simulations under fixed cell conditions using each of the reported lattice parameters. From these simulations, further analysis and simulations were performed on the lowest enthalpy struc-

TABLE I. Relative enthalpies and symmetry information of the six lowest enthalpy phases found from genetic algorithm based structure searches for cell A.

	Fixed Cell[a]		Variable Cell[b]			
Structure	Enthalpy (eV/atom)	Symmetry	Enthalpy (eV/atom)	Symmetry	Lattice ratios $(a/b, a/c)$	Lattice angles (α, β, γ)
A1	0.0	$P2_1/C$	0.0	*Pbcn*	1.59, 0.87	90,90,90
A2	0.185	$P2_12_12_1$	0.056	$P2_12_12_1$	1.44, 0.77	90,90,90
A3	0.330	*Cmca*	0.051	*Cmca*	1.24, 0.86	90,90,90
A4	0.451	*PC*	−0.001	$P2_1/C$	1.59, 0.80	90,69,90
A5	0.424	$P2_1/C$	0.042	*Cmcm*	1.50, 0.75	82,90,90
A6	0.545	*P*-1	0.047	*P*-1	1.45, 0.74	79,97,89
Expt.[c]					1.50, 0.83	90,90,90

[a]Structural search using experimentally determined lattice parameters.
[b]Results correspond to structures from the fixed cell structure search that have been optimized where the cell and ion positions are allowed to relax.
[c]Reference 12.

tures with the goal of elucidating the ζ-phase structure from each of the reported lattice parameters.

A. Cell A

For cell A (Ref. 12) the proposed lattice parameters were $a=4.159$, $b=2.765$, and $c=5.039$ at 80 GPa for an eight-atom orthorhombic unit cell with either $P222_1$, $P2_12_12$, or $P2_12_12_1$ symmetry. Using this cell, seven separate genetic algorithm (GA) structure searches were performed at the DFT level of theory. The six lowest-energy structures recovered from the search are shown in Table I, labeled as structures A1–A6.

The enthalpy of each structure is reported relative to the lowest enthalpy structure A1, which was recovered from all seven GA structure searches. Structure A1 is 0.185 eV/atom more stable than the next most stable structure, but its $P2_1/C$ symmetry does not correspond to any symmetries assigned to cell A. The next lowest enthalpy structure A2, however, possesses $P2_12_12_1$ symmetry, one of the proposed space groups for cell A. Geometries of structures A1 and A2 are shown in Figs. 1(a) and 2(a), respectively. The remaining low enthalpy structures (A3–A6) lie at least 0.330 eV/atom higher than A1 and none have the symmetries that were experimentally assigned to cell A. The calculated powder x-ray diffraction patterns for structures A1 and A2 are shown in Figs. 3(a) and 3(b), respectively, with the experimental peak positions and relative intensities also shown. The peak indices of both structures match up well with experiment, showing peaks at 9.6°, 10°, 10.5°, 11.2°, 11.5°, 11.6°, and 12.6°. However the relative peak intensities are not as well-matched.

Structures A1–A6 from the GA structure search were allowed to fully relax with the cell constraints released during optimization, permitting the trace of the stress tensor to match the experimental pressure of 80 GPa. The enthalpies, lattice parameters, and symmetry assignments of the relaxed structures are reported on the right-hand side of Table I. Following full relaxation, the spread in the enthalpy of structures A1–A6 diminishes from 0.545 eV/atom to 0.056 eV/atom. Moreover, structure A4 becomes the lowest enthalpy phase by a small margin over A1. However, A4 also becomes monoclinic following relaxation and is therefore not compatible with cell A. Structures A5 and A6 also relax to non-orthorhombic unit cells. Noting that molecular nitrogen itself is metastable at these ultrahigh pressures, we will not discuss structures A4–A6 due to their incompatibility with the experimental cell. The relaxed A3 structure lies only 0.05 eV/atom above structure A1 and maintains the orthorhombic unit cell. However, the *Cmcm* symmetry of structure A3 does not have many common symmetry elements to the proposed experimental symmetries and therefore structure A3 was not considered further.

Herein, we will focus on structures A1 and A2 since they remain among the lowest enthalpy phases and they experience the least change in their cell parameters upon full relaxation at 80 GPa. For example, their respective cells remain orthorhombic and their lattice vector ratios remain within 7% of the experimental parameters. Structure A2 re-

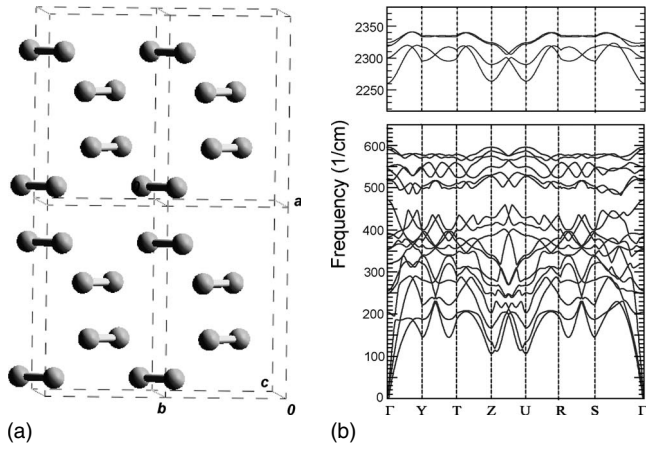

FIG. 1. (a) $2\times2\times2$ supercell of structure A1 following variable cell optimization. (b) phonon dispersion curves for structure A1 in the lattice and vibrational regions.

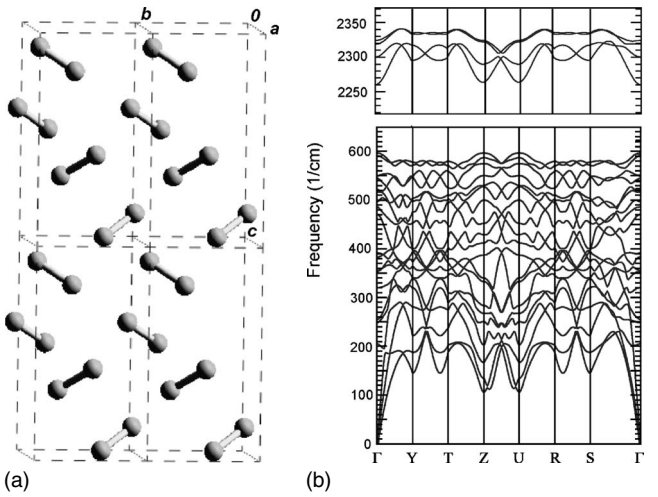

FIG. 2. (a) $2\times2\times2$ supercell of structure A2 following variable cell optimization. (b) Phonon dispersion curves for structure A2 in the lattice and vibrational regions.

tains $P2_12_12_1$ symmetry whereas the higher-symmetry A1 structure adopts *Pbcn* symmetry, which can be related to the $P2_12_12$ space group by adding the appropriate glide plane symmetry elements. The structural details of A1 and A2 are given in Table II. Figure 4 shows the calculated enthalpies of select molecular phases relative to the polymeric cg-N structure plotted as a function of pressure. Structures A1 and A2 are included among them along with the molecular α and ε phases. As expected, the cg-N structure becomes thermodynamically favored above 50 GPa.[26] Structures A1 and A2 are both lower in enthalpy than either the molecular α or ε phases in the 70–90 GPa pressure range, wherein the enthalpy-pressure curve for structure A2 crosses that of the ε phase near 68 GPa.

Phonon dispersion curves for the optimized A1 and A2 structures at 80 GPa are given in Figs. 1(b) and 2(b), respectively. These curves show that there are no negative phonon modes, confirming both phases are mechanically stable at 80 GPa. Comparison with phonon dispersion curves at 30 and 50 GPa show a softening of the lowest phonon with decreasing pressure, suggesting an instability in the structure as the pressure is relieved. This behavior is expected of high-pressure molecular phases of nitrogen. Calculated equations of state for both structures and the cg-N structure are shown in Fig. 5. At 110 GPa, the ζ to cg-N transition is predicted to exhibit a large volume drop of 24.7% and 23.4% for the A2 and A1 phases, respectively, which correlates well with the experimentally observed volume drop of 22%.[12]

Experimentally, Eremets *et al.*[12] reported that the Raman modes were weak and difficult to interpret for cell A. By visual inspection of the number of bands in the N-N vibrational region of the calculated phonon spectra at the gamma point, we can obtain an upper bound on the number of available vibrational Raman modes. It can be seen that both structures A1 and A2 have four available vibrational modes, which can be reduced to three if we consider frequencies within 10 cm^{-1} to be degenerate. There have been reports of high-pressure phases of molecular nitrogen in which only three active Raman modes were observed for an "anomalous" ζ phase at 74 GPa.[7] Hemley and co-workers reported five Raman active N-N vibrational modes experimentally for cell B. We propose either A1 or A2 is the ζ phase characterized in cell A,[12] but, in light of the arguments given above, it is difficult to definitively assign one structure over the other. Additional experiments and refinements may be required to obtain an unambiguous determination of the ζ phase structure.

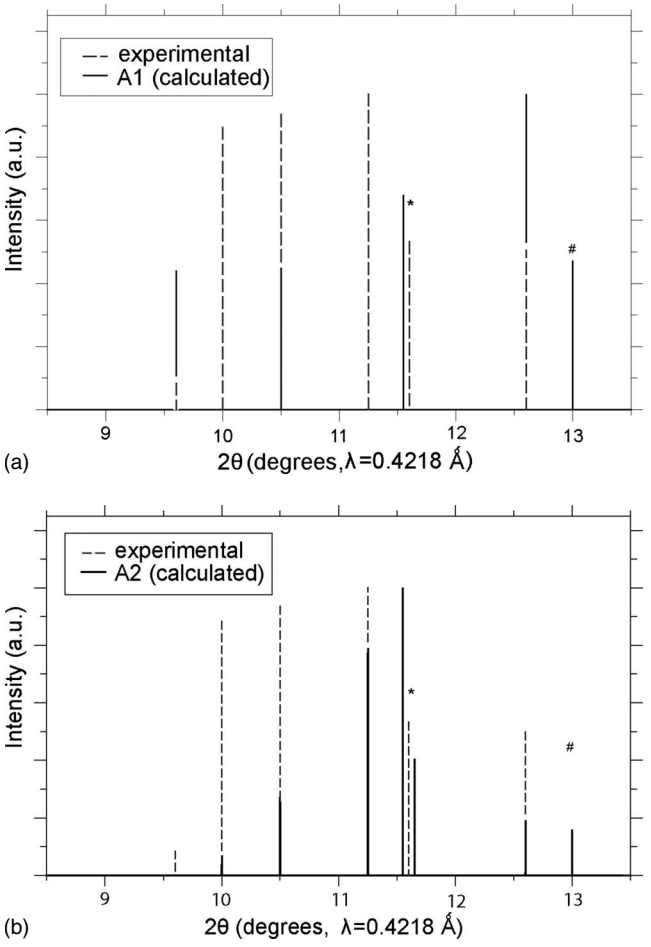

FIG. 3. Calculated x-ray diffraction patterns (solid) of structures (a) A1 and (b) A2 compared to the experimental diffraction pattern reported in Ref. 12 (dashed). Intensities, shown in arbitrary units, are scaled such that the most intense peaks overlap fully. For the peaks labeled as "*" only one peak is seen experimentally at ~11.6° with one Bragg angle position on either side. The peak labeled "#" at 13.0° is found in experiment.

B. Cell B

For cell B (Ref. 10) the reported lattice parameters are $a=6.533$, $b=2.576$, and $c=6.844$ at 90 GPa for a 16 atom orthorhombic unit cell. Unlike cell A, the symmetry for cell B was reported to be *Pmma* (Ref. 10) and one lattice vector in cell B is substantially shorter than the other two. This would tend to favor crystal molecular structures that adopt molecular orientations perpendicular to the short lattice vector, otherwise the crystal would likely adopt a chain structure

TABLE II. The unit-cell parameters and atomic positions of selected structures from the first-principles genetic algorithm based structure search.

Structure	Space group	*a* (Å)	*b* (Å)	*c* (Å)	*Z* [a]	Atoms	*x*	*y*	*z*
A1[b]	*Pbcn*	2.680	4.249	4.908	4	N1	0.3662	0.8629	0.6640
A2[b]	$P2_12_12_1$	3.964	2.746	5.196	4	N1	0.7833	0.2502	0.178
						N2	0.6466	0.9586	0.0739
B1[c]	*Immm*	3.450	2.965	2.636	2	N1	0.6614	0.0	0.0
B8[c]	*Pnma*	5.249	7.857	2.640	8	N1	0.5795	0.5011	0.6377
						N2	0.1232	0.7500	0.6294
						N3	0.7822	0.7500	0.1471

[a]Number of N_2 molecules per unit cell.
[b]Structures optimized at 80 GPa.
[c]Structures optimized at 90 GPa.

and effectively break the molecular triple bond to reconcile the intermolecular repulsion.

Using cell B, the GA structure search was applied with its reported experimental cell parameters. Examples of the lowest enthalpy molecular structures derived from cell B are reported in Table III, labeled B1–B6. Most of the structures that were generated possessed no symmetry with the notable exception of the lowest enthalpy structure B1 which possesses *Pmma* symmetry, the same as that assigned experimentally. Structures B2–B6 correspond to selected examples of the lowest-enthalpy low-symmetry molecular structures.

The geometry of structure B1 is shown in Fig. 6(a). The simulated x-ray powder diffraction pattern (not shown) for the B1 structure shows sharp peaks at 10° and 12°. Although the peaks at 10° and 12° become the predominant peaks at high pressures,[10] there are additional peaks observed experimentally. This is perhaps indicative of a forced alignment of the highly strained molecules as the pressure is increased. Nonetheless, the additional peaks seen in experiment below 10° and between 10° and 12° are notably absent in structure B1.

The atomic structures and cell vectors of structures B1–B6 were fully optimized. Upon cell relaxation, structures B2–B6 still possessed no symmetry and remained higher in enthalpy than structure B1. Structure B1 remained orthorhombic after cell relaxation and the a/b and a/c lattice ratios of the 16 atom simulation cell remained within 5% of the experimental values. But it was found that the simulation cell of structure B1 could be reduced to a four atom unit cell with *Immm* symmetry. This contrasts sharply with the 16 atom unit cell and lower *Pmma* symmetry reported experimentally. Interestingly, the optimized B1 structure was found to be closely related to a recently reported *Immm* phase[33] of polynitrogen, which those authors obtained by optimizing coordinates of the recently solved ε phase of high-pressure

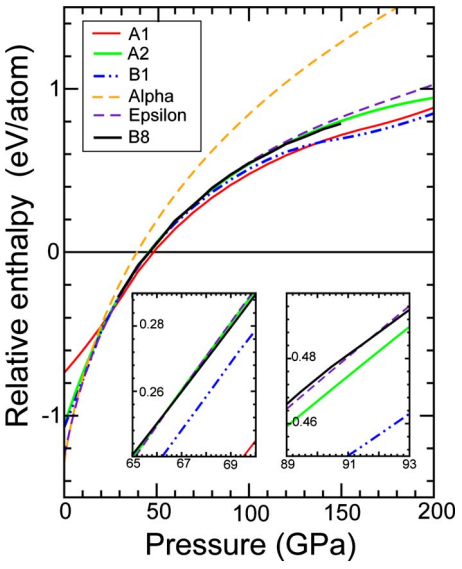

FIG. 4. (Color online) Relative enthalpy versus pressure phase diagram for structures A1, A2, B1, and B8, and the α and ε phases of molecular nitrogen. Enthalpies are referenced to the cg-N structure. The two insets show the crossover of the ε phase with structures A2 and B8 between 65–69 GPa (left inset) and with B8 at ~91 GPa (right inset).

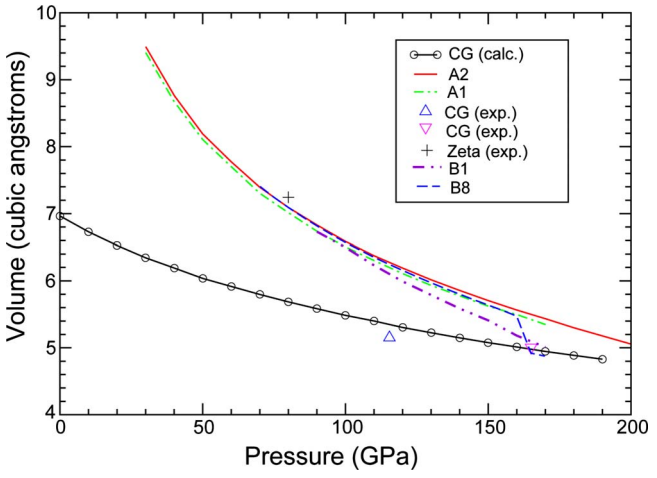

FIG. 5. (Color online) Calculated pressure-volume relations for cg-N (solid line with open circles), structure A1 (solid line), structure A2 (dashed-dotted line), structure B1 (dashed-dotted-dotted line), and structure B8 (dashed line). Experimental *PV* relations from Ref. 15 (blue triangle), Ref. 12 (black cross), and Ref. 10 (pink inverted triangle) are also shown.

TABLE III. Relative enthalpies and symmetry information of the low enthalpy phases generated from genetic algorithm based structure searches for cell B.

	Fixed cell[a]		Variable cell[b]			
Structure[c]	Enthalpy (eV/atom)	Symmetry	Enthalpy (eV/atom)	Symmetry	Lattice ratios $(a/b, a/c)$	Lattice angles (α, β, γ)
B1	0.0	*Pmma*	0.0	*Immm*	1.11, 2.69	90, 90, 90
B2	0.085	*P*1	0.008	*P*1	1.02, 2.43	90, 92, 90
B3	0.154	*P*1	0.029	*P*1	1.11, 2.54	90, 90, 84
B4	0.169	*P*1	0.027	*P*1	1.01, 2.43	88, 93, 87
B5	0.227	*P*1	0.018	*P*1	1.04, 2.46	100, 84, 95
B6	0.315	*P*1	0.050	*P*1	1.11, 2.52	98, 94, 94
B7	0.363	*Pmma*	–0.041	$P2_1/C$	1.41, 2.86	90, 96, 90
B8	0.485	*Pmma*	0.019	*Pnma*	1.50, 2.97	90, 90, 90
B9	0.398	*Pmma*	0.368	*Pmma*	1.07, 2.91	90, 90, 90
B10[d]	0.415	*Pmma*	0.0[d]	*Immm*	1.11, 2.69	90, 90, 90
Expt.[e]		*Pmma*			1.05, 2.66	90, 90, 90

[a]Structural search using experimentally determined lattice parameters.
[b]Results correspond to structures from the fixed cell structure search that have been optimized where the cell and ion positions are allowed to relax.
[c]Structures B1–B6 are derived a symmetry unrestricted search, whereas structures B7–B10 are derived from a *Pmma* space group restricted search as described in the text.
[d]Upon cell relaxation, structure B10* optimized to structure B1.
[e]Reference 10.

molecular oxygen.[1,2] To explore the space-group discrepancy further and reinforce the notion that we had explored the region of the potential-energy surface with *Pmma* symmetry, we modified our structure searching algorithm to exclusively generate initial structures with *Pmma* symmetry by placing the atoms on Wyckoff sites of the *Pmma* space group in a 2/1/1 distribution, as explained in Ref. 9.

With this "symmetry restricted" GA search, structure B1 again emerged as the lowest enthalpy structure using the experimental cell parameters. Four of the remaining lower enthalpy structures are presented in Table III, labeled as structures B7–B10. Within the experimental cell parameters, structures B7–B10 were at least 0.363 eV/atom higher in enthalpy than B1.

Upon full optimization where the cell parameters are allowed to relax, structure B10 optimized to structure B1. This, and the fact that B1 adopts *Immm* symmetry from *Pmma* symmetry upon cell relaxation, shows that the *Immm* and *Pmma* structures can be related by simply rotating some of the molecules out of the plane of the two largest lattice vectors. These distortions may manifest themselves within an imperfect crystal.

Structure B7 emerged as the lowest enthalpy structure when the cell constraints were released during the optimization procedure. However the structure assumes a monoclinic representation, deviating from the desired orthorhombic symmetry, and was subsequently not examined further. Although structure B9 maintains an orthorhombic unit cell, the relaxed structure remains significantly higher in enthalpy than B1. Moreover, a phonon dispersion calculation of structure B9 (following relaxation) revealed that it was not mechanically stable at 90 GPa and therefore was not considered further. Although unspectacular when constrained to the fixed experimental cell, structure B8 [shown in Fig. 7(a)] emerges as another low enthalpy phase. Encouragingly, it has an orthorhombic 16 atom unit cell with *Pnma* symmetry, which is only slightly higher in symmetry than the experimentally assigned *Pmma* symmetry.

From the above results, structures B1 and B8 are considered as the lead candidate structures for cell B. Figure 4 shows that at 90 GPa, structure B1 is lower in enthalpy than both the α and ε molecular phases. While B8 is lower in enthalpy than the α phase, it only becomes more enthalpically stable than ε at pressures between 67 and 76 GPa and pressures greater than ~91 GPa. Phonon dispersion curves for structures B1 and B8, given in Figs. 6(b) and 7(b), respectively, show that both phases are mechanically stable at 90 GPa. Although the phonon dispersion curves of B8 show no negative frequency modes, Fig. 7(b) reveals there is a very weak mode between the Γ and X symmetry points that dips as low as 6 cm^{-1}. The calculated pressure versus volume curves in Fig. 5 show structure B8 undergoes a phase transformation near 160 GPa, accompanied by a notable decrease in volume. At this point structure B8 transforms into a two dimensional polymeric chainlike phase. Structure B1 undergoes a phase transformation at ~150 GPa to a phase with *I*4*mmm* symmetry. Though its volume is close to that of cg-N polymeric nitrogen, the *I*4*mmm* structure is still a molecular phase. Hemley *et al.*[33] reported that a simple distortion of their proposed *Immm* phase of polynitrogen can describe its transformation to the highly sought cg-N structure.[16]

Although the simplistic structure of structure B1 is appealing, it clearly has a four atom unit cell which contrasts

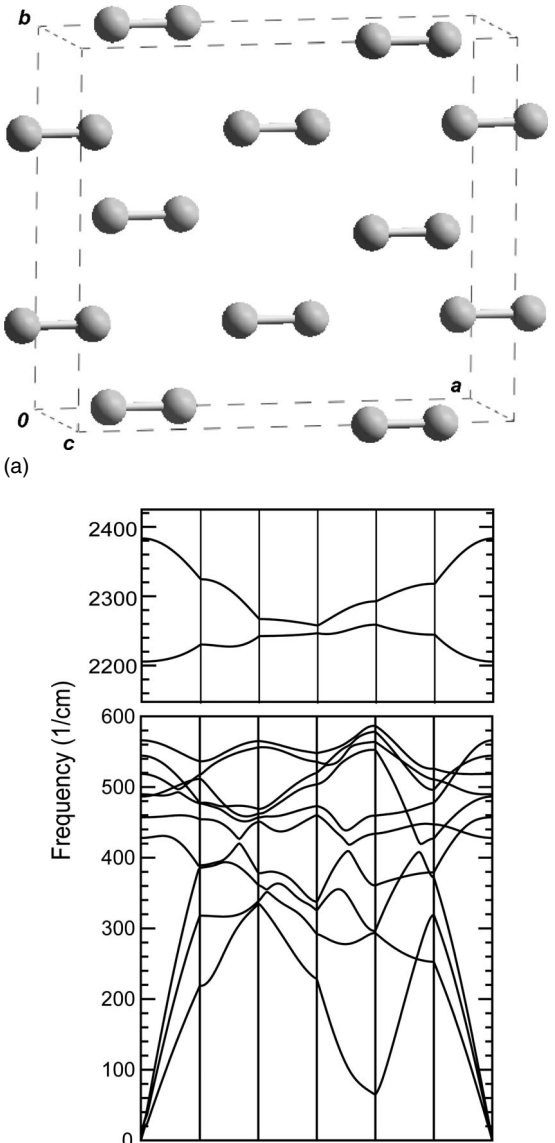

FIG. 6. (a) 16 atom cell representation of structure B1 following variable cell optimization. (b) Phonon dispersion curves for structure B1 at 90 GPa in the lattice and vibrational regions.

sharply with the 16 atom cell identified experimentally. Furthermore, the *Immm* symmetry of structure B1 has four atoms occupying 4*e* Wyckoff sites. This allows for only two Raman bands in the molecular vibration region of the spectrum, whereas five Raman bands were clearly identified for cell B.[9] Alternatively, structure B8 only lies 0.019 eV/atom higher in enthalpy than B1 at 90 GPa and has the desired 16 atom unit cell. Furthermore, its *Pnma* symmetry is close to the experimentally identified *Pmma* symmetry. Structure B8 is also more consistent with the experimental Raman data of cell B. Its atoms are distributed among 8*d* and 4*c* Wyckoff sites, allowing the desired five Raman stretching components. Also, the 2/1/1 distribution of molecules over wyckoff sites supports the redistribution of vibrational intensities at the ε-ζ phase transition.[9] However, the a/b lattice vector ratio for structure B8 is 44% larger than that determined experimentally. Despite the larger lattice vector ratio, we

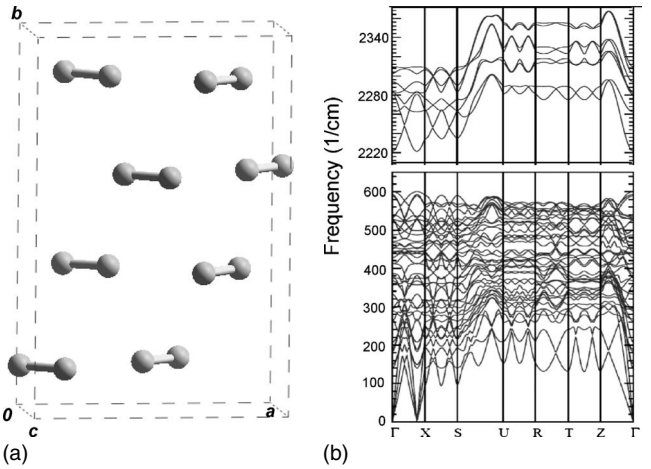

FIG. 7. (a) Unit cell representation of structure B8 (following variable cell optimization). (b) Phonon dispersion curves for structure B8 at 90 GPa in the lattice and vibrational regions

consider that structure B8 is the best candidate structure resulting from our GA/DFT calculations for cell B because it is more consistent with the experimental symmetry and Raman data than B1.

IV. CONCLUSIONS

We have performed an exhaustive genetic algorithm search at the first-principles DFT level of the high-pressure ζ phase of nitrogen using two sets of experimentally reported lattice parameters. For the lattice parameters reported by Eremets and co-workers determined at 80 GPa,[12] we find two competitive structures that we have labeled A1 and A2. Their optimized cell parameters remained close to the experimental values and phonon dispersion calculations showed that both structures are mechanically stable. Structure A1 is the lowest enthalpy of the two aforementioned phases, but its *Pbcn* symmetry does not match the proposed symmetry analysis.[12] However, it possesses many of the required symmetry elements and is closely related to the experimentally proposed candidate $P2_12_12$ space group. Conversely, structure A2, with its $P2_12_12_1$ symmetry, agrees with the proposed symmetry analysis and has a more common symmetry than *Pbcn*, but it is higher in enthalpy.

For the lattice parameters of the molecular ζ-phase structure reported by Hemley and co-workers at 90 GPa,[10] we also find two competitive structures labeled B1 and B8. Both structures are calculated to be mechanically stable at 90 GPa. Although structure B1 is 0.019 eV/atom lower in enthalpy than B8 at 90 GPa, we consider structure B8 to be a stronger candidate for the ζ-phase reported by Hemley and coworkers for several reasons. First, structure B1 has a 4 atom unit cell, whereas both the experimental and B8 unit cells have 16 atoms. Furthermore, the *Pnma* symmetry of structure B8 is significantly closer to the experimentally identified *Pmma* symmetry as compared to the *Immm* symmetry of B1. Finally, structure B8 is more consistent with the experimental Raman data which is reported to have five bands in the N-N stretching region. The distribution of molecules at the

Wyckoff sites for B1 only allows for two Raman bands in this region whereas the symmetry of structure B8 allows for five.

The conflicting experimental reports and our own calculations, having found dozens of local minima on the molecular potential-energy surface, reinforce the notion that the phase diagram of nitrogen is quite rich and complex between 80 and 90 GPa. Our results support the existence of multiple near-degenerate history-dependent structures of high-pressure molecular nitrogen, such as structures A1 and B1. Since the samples are under tremendous strain experimentally, the "true" structures are likely highly distorted in the diamond anvil cell environment, this would explain the problems associated with characterizing the ζ molecular phase structure. Being a supposed precursor to the cubic gauche phase, the true structure of the ζ molecular phase or an understanding of that region of the phase diagram could prove invaluable in assessing the feasibility of polymeric nitrogen.

ACKNOWLEDGMENTS

We thank Defense Research and Development Canada-Suffield, NSERC and the Canada Research Chairs program for funding. We are also grateful to CFI, the Ontario Research Fund, and IBM Canada for providing computing resources.

*Corresponding author; twoo@uottawa.ca

[1] L. F. Lundegaard, G. Weck, M. I. McMahan, S. Desgreniers, and P. Loubeyre, Nature (London) **443**, 201 (2006).
[2] H. Fujihisa, Y. Akahama, H. Kawamura, Y. Ohishi, O. Shimomura, H. Yamawaki, M. Sakashita, Y. Gotoh, S. Takeya, and K. Honda, Phys. Rev. Lett **97**, 085503 (2006).
[3] Y. Ma, A. R. Oganov, and C. W. Glass, Phys. Rev. B **76**, 064101 (2007).
[4] G. Weck, S. Desgreniers, P. Loubeyre, and M. Mezouar, Phys. Rev. Lett. **102**, 255503 (2009).
[5] M. I. M. Scheerboom and J. A. Schouten, J. Chem. Phys. **105**, 2553 (1996).
[6] R. Bini, M. Jordan, L. Ulivi, and H. J. Jodl, J. Chem. Phys. **108**, 6849 (1998).
[7] H. E. Lorenzana, M. J. Lipp, and W. J. Evans, High Press. Res. **22**, 5 (2002).
[8] M. J. Lipp, J. P. Klepeis, B. J. Baer, H. Cynn, W. J. Evans, V. Iota, and C. S. Yoo, Phys. Rev. B **76**, 014113 (2007).
[9] E. Gregoryanz, C. Sanloup, R. Bini, J. Kreutz, H. J. Jodl, M. Somayazulu, H.-k. Mao, and R. J. Hemley, J. Chem. Phys. **124**, 116102 (2006).
[10] E. Gregoryanz, A. F. Goncharov, C. Sanloup, M. Somayazulu, H.-k. Mao, and R. J. Hemley, J. Chem. Phys. **126**, 184505 (2007).
[11] H. Katzke and P. Toledano, Phys. Rev. B **78**, 064103 (2008).
[12] M. I. Eremets, A. G. Gavriliuk, N. R. Serebryanaya, I. A. Trojan, D. A. Dzivenko, R. Boehler, H. K. Mao, and R. J. Hemley, J. Chem. Phys. **121**, 11296 (2004).
[13] R. Bini, L. Ulivi, J. Kreutz, and H. J. Jodl, J. Chem. Phys. **112**, 8522 (2000).
[14] K. Shimizu, K. Suhara, M. Ikumo, M. I. Eremets, and K. Amaya, Nature (London) **393**, 767 (1998).
[15] M. I. Eremets, A. G. Gavriliuk, I. A. Trojan, D. A. Dzivenko, and R. Boehler, Nature Mater. **3**, 558 (2004).
[16] C. Mailhiot, L. H. Yang, and A. K. McMahan, Phys. Rev. B **46**, 14419 (1992).
[17] D. M. Deaven and K. M. Ho, Phys. Rev. Lett. **75**, 288 (1995).
[18] Y. Zeiri, Phys. Rev. E **51**, R2769 (1995).
[19] A. R. Oganov, C. W. Glass, and S. Ono, Earth Planet. Sci. Lett. **241**, 95 (2006).
[20] A. R. Oganov and C. W. Glass, J. Chem. Phys. **124**, 244704 (2006).
[21] Y. Ma, M. I. Eremets, A. R. Oganov, Y. Xie, I. A. Trojan, S. Medvedev, A. O. Lyakhov, M. Valle, and V. Prakapenka, Nature (London) **458**, 182 (2009).
[22] Q. Li, Y. Ma, A. R. Oganov, H. Wang, H. Wang, Y. Xu, T. Cui, H. K. Mao, and G. Zou, Phys. Rev. Lett. **102**, 175506 (2009).
[23] G. Gao, A. R. Oganov, A. Bergara, M. Martinez-Canales, T. Cui, T. Iitaka, Y. Ma, and G. Zou, Phys. Rev. Lett. **101**, 107002 (2008).
[24] Y. Yao, J. S. Tse, and K. Tanaka, Phys. Rev. B **77**, 052103 (2008).
[25] Y. Ma, A. R. Oganov, Z. Li, Y. Xie, and J. Kotakoski, Phys. Rev. Lett. **102**, 065501 (2009).
[26] J. Kotakoski and K. Albe, Phys. Rev. B **77**, 144109 (2008).
[27] G. Kresse and J. Furthmuller, Phys. Rev. B **54**, 11169 (1996).
[28] P. E. Blochl, Phys. Rev. B **50**, 17953 (1994).
[29] J. P. Perdew, K. Burke, and M. Ernzerhof, Phys. Rev. Lett. **77**, 3865 (1996).
[30] A. Togo, F. Oba, and I. Tanaka, Phys. Rev. B **78**, 134106 (2008).
[31] J. M. Soler, E. Artacho, J. D. Gale, A. Garcia, J. Junquera, P. Ordejon, and D. Sanchez-Portal, J. Phys.: Condens. Matter **14**, 2745 (2002).
[32] *Materials Studio Modeling* (Accelyrs Software Inc., San Diego, 2005), Vol. 3, p. 2.
[33] R. Caracas and R. J. Hemley, Chem. Phys. Lett. **442**, 65 (2007).